The 2009 IEEE/RSJ International Conference on
Intelligent Robots and Systems
October 11-15, 2009 St. Louis, USA

Haptic Display of Realistic Tool Contact Via Dynamically Compensated Control of a Dedicated Actuator

William McMahan and Katherine J. Kuchenbecker

Abstract— **High frequency contact accelerations convey important information that the vast majority of haptic interfaces cannot render. Building on prior work, we present an approach to haptic interface design that uses a dedicated linear voice coil actuator and a dynamic system model to allow the user to feel these signals. This approach was tested through use in a bilateral teleoperation experiment where a user explored three textured surfaces under three different acceleration control architectures: none, constant gain, and dynamic compensation. The controllers that use the dedicated actuator vastly outperform traditional position-position control at conveying realistic contact accelerations. Analysis of root mean square error, linear regression, and discrete Fourier transforms of the acceleration data also indicate a slight performance benefit for dynamic compensation over constant gain.**

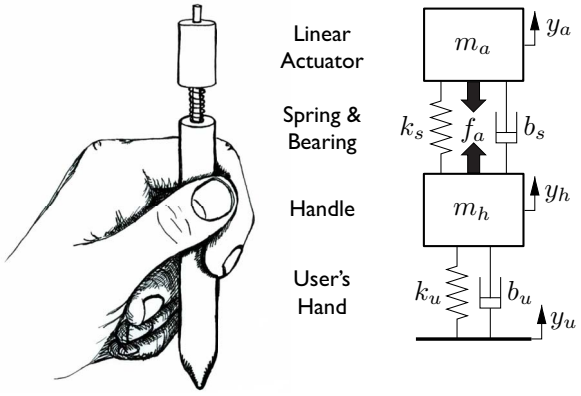

Fig. 1. Conceptual model and mass-spring-damper diagram for the use of a dedicated linear actuator in creating high frequency handle accelerations.

I. INTRODUCTION

When using a tool to touch an object, you can feel a rich array of haptic cues that reveal the state of the interaction as well as rich details of the item's geometry, material, and surface properties [9], [16], [10]. For example, the vibrations and forces experienced by your hand as you draw on a bumpy piece of cardboard are distinct from those generated when using a wrench to tighten a metal nut or using a scalpel to make a surgical incision. The human talent for discerning haptic surface properties such as stiffness and texture through an intermediate tool stems partly from the phenomenon of distal attribution, in which a hand-held tool comes to feel like an extension of one's own body [19]. Humans are highly adept at interpreting the haptic feedback that arises during these tool-mediated interactions, effortlessly using this information to accomplish the activities of daily living as well as the feats of exceptional dexterity seen in art, manufacturing, surgery, and many other professions.

Haptic interfaces are computer-controlled electromechanical systems that enable a human user to feel and manipulate virtual or remote environments. Commercial haptic interfaces are typically lightweight, backdrivable robot arms. These devices measure the motion of a tool as it is moved by the user's hand and apply forces and torques in response. In the virtual domain, the most promising current applications for haptic interface technology include interactive medical simulators that allow doctors to practice new procedures before attempting them on human patients; digital sculpture and design systems that enable users to intuitively create and explore three-dimensional shapes before they are physically realized; and immersive games that give users an immediate feel for simulated events such as collisions. For remote interactions, haptic interfaces are being extensively researched for robot-assisted minimally invasive surgery and control of robots in hazardous environments, such as the deep sea or a military battlefield. These haptic interface systems all focus on providing the user with haptic feedback that can mimic the sensations experienced during tool-based interactions with the real world.

Unfortunately, almost all existing haptic virtual environments are programmed with simple position-force relationships that strongly resemble algorithms that were developed more than fifteen years ago, e.g., [23]. We hypothesize that such an approach does not capture the richness of real interactions with hard and textured objects, because the 20 to 1000 Hz accelerations that distinguish these contacts will be missing. Evidence for this hypothesis can be found in a human subject study conducted by Kuchenbecker and colleagues [13] that demonstrated that typical virtual surfaces seeking to emulate the feel of *wood* are actually indistinguishable from *soft foam*, earning a mere two out of seven for realism during unsighted exploration. As depicted in the left half of Fig. 1, we propose a new method for achieving high-fidelity haptic feedback that feels like real contact. Our method uses a dedicated high frequency vibration actuator and dynamically compensated control to complement the low frequency forces provided by a typical grounded haptic interface.

II. BACKGROUND

Haptic properties such as stiffness, friction, and texture are almost always programmed by hand via simple parametric

This work was supported by the University of Pennsylvania.

W. McMahan is with the Department of Mechanical Engineering and Applied Mechanics, University of Pennsylvania, Philadelphia, PA 19104, USA, wmcmahan@seas.upenn.edu

K. J. Kuchenbecker is with the Faculty of the Department of Mechanical Engineering and Applied Mechanics, University of Pennsylvania, Philadelphia, PA 19104, USA, kuchenbe@seas.upenn.edu

relationships between tool position and/or velocity and the force to be output by the haptic interface's motors. The time-consuming, subjective nature of this tuning process does not extend well to the creation of haptic environments that contain a broad assortment of simulated objects, nor does it generally yield virtual environments that feel compellingly like their real counterparts. Though one can increase the range of impedances that can be rendered with a traditional haptic interface by maximizing inherent damping, sensor resolution, and sampling rate [2], the improvements that would be required to render the feel of a wooden block or a piece of sandpaper with this approach are beyond the range of current technology [6]. Faced with this limitation, researchers have started finding ways to approach the realism of natural physical interactions by instilling their virtual environments with auxiliary high frequency feedback that resembles the signals encountered in real-world interactions.

In some prior work, e.g., [22], [21], [8], [3], [13], [14], contact vibration transients were added to traditionally rendered surfaces using the haptic interface's native actuators, which are typically brushed DC motors. This technique is attractive because it provides higher bandwidth stimulation for the user without requiring any additional hardware. Such an approach is an improvement over position-based feedback alone, but it is highly susceptible to configuration-based variations in the device's high frequency dynamics. As a result a transient played in one direction or one location in the workspace can feel different from the same transient played in a different direction and/or location. Furthermore, there are limits to the quality and magnitude of the signals that can be created in this way. This is especially significant at high frequency where haptic interfaces typically have considerable signal attenuation and lag, and where discrete-time sampling effects and actuator saturation are compounding factors.

A viable alternative rendering paradigm can be found in the older teleoperation work of Howe and colleagues, where high frequency slave fingertip accelerations were relayed to the user (along with low frequency force feedback) via a pair of supplementary voice coil actuators [11], [12]. The measured acceleration was multiplied by an empirically determined constant to drive the actuator, and the authors reported that its output varied by a factor of 2.24 across the frequency range of interest. Despite the simplicity of this approach, human subject tests indicated that this hybrid feedback strategy increased user performance in inspection, puncturing and peg-in-slot tasks. Furthermore, users commented that the vibrations improved the "feel" of the interface. Later work improved the strength of the vibration actuator for better rendering of contact transients in the absence of position-based feedback [5]. Wellman and Howe used this same approach to add exponentially decaying sinusoid transients to virtual surfaces [26], though their vibrational output was not more carefully controlled than that of Kontarinis and Howe.

Despite the encouraging open-loop output results of Howe and colleagues, few researchers and no haptic device companies have chosen to use a supplementary vibration actuator for high-fidelity haptic rendering; this slow adoption rate may stem from the current lack of rich haptic contact models, the technical difficulty and expense of adding extra input and output channels to a device, or other barriers that are not yet understood. While several groups have created active styli meant to be used without a force-feedback device [27], [17], [18], the only pertinent hybrid example that could be located in the literature is Wall and Harwin's vibrotactile display stylus, which was developed to study the perception of device output bandwidth on virtual grating perception [25], [24]. This design places a voice coil actuator between the stylus and the end-effector of a desktop haptic device, and they control its displacement using high-resolution measurements from a parallel LVDT sensor. The associated human-subject study found that the active probe's high frequency feedback significantly reduced the spatial period threshold for discrimination of virtual grating orientations over an unaugmented device. Although this finding supports the efficacy of the supplementary actuator approach, the authors and subjects noted a major drawback to this stylus design: the chosen placement of the voice coil actuator introduces a highly compliant element between the hand and the desktop haptic device. This design element diminishes the renderable surface stiffnesses to levels even further below those encountered in everyday objects. In contrast to this prior work, our proposed active stylus design is innovative because it capitalizes on the benefits of a supplementary voice coil actuator without introducing this compliance.

III. TECHNICAL APPROACH

Human haptic sensory and motor capabilities are inherently asymmetric [4], allowing controlled motion at just 8 to 10 Hz [20] and vibration perception up to 1000 Hz [1]. To achieve unprecedented levels of haptic realism, we seek to create haptic interfaces that appropriately complement this human asymmetry by accurately generating a rich range of vibrations at the user's fingertips.

A. Haptic Interface Design

Our proposed haptic interface requires an actuator that has both the strength and bandwidth to induce accelerations at the magnitude and frequency of tool-mediated contact tasks. It is also important that the amplitude and frequency of the force are independently controllable and that the actuator can generate accelerations in both the positive and the negative axial directions. For these reasons, we ruled out eccentric mass motors and solenoids and selected a voice coil actuator. As shown in Fig. 1, our design concept attaches a voice coil actuator to the handle of a typical impedance-type haptic interface through a linear bearing and a recentering spring. This high-bandwidth actuator is thus collocated with the output we want to control, i.e., handle acceleration, a_h. Furthermore, we aim to explicitly measure this output signal in real time so that the quality of the user's experience can be monitored and modulated across changing configurations of the haptic device and the user's hand.

At this point, it is important to note the benefits of targeting acceleration feedback rather than force feedback.

Force sensors are large, fragile, and expensive, and must be mounted between two mechanical components (such as the handle and the haptic interface) in order to provide useful measurements. In contrast, MEMS-based accelerometers are very small, robust, affordable, and can be rigidly mounted to the outside of an object to observe its motion. We believe that virtual environments and teleoperated robots should be designed to provide users with a desired high frequency acceleration at the handle, which can be overlaid on the low frequency force feedback available from the interface's base-mounted motors. One could potentially employ three such voice coil actuators in an orthogonal configuration for independent control of each axis of tool tip acceleration; we seek to create a good single-axis device before exploring whether three actuation axes are required.

The behavior of this dedicated actuator can be understood by examining the dynamics that couple its force output, f_a, to observed handle acceleration, a_h. The system can be parametrically modeled by the configuration of masses, springs, and dampers shown in the right half of Fig. 1. The handle mass, m_h, is held in the user's hand, which is modeled as a spring and a damper connected to the user's desired position, y_u. This second-order model has previously been shown to capture the behavior of the human hand holding a tool, with the effective stiffness (k_u) and damping (b_u) both increasing with grip force and changing somewhat with hand configuration [15], [7]. To enable the user to feel high frequency accelerations at their fingertips, we attach a linear actuator with mass, m_a, to the handle. It can pull the two masses together (or push them apart) with equal and opposite forces of magnitude, f_a. The actuator is recentered by a spring, k_s, and the friction in its linear bearings acts as a damper, b_s, in parallel with the spring. We can write the equations of motion for both masses, rearrange, and take the Laplace transforms to yield the following pair of coupled ordinary differential equations:

$$(m_a s^2 + b_s s + k_s) Y_a(s) = -F_a(s) + (k_s + b_s s) Y_h(s) \quad (1)$$

$$\begin{aligned} \left(m_h s^2 + (b_s + b_u)s + (k_s + k_u)\right) Y_h(s) = \\ F_a(s) + (k_s + b_s s) Y_a(s) + (k_u + b_u s) Y_u(s) \end{aligned} \quad (2)$$

We know that the user's desired position (y_u) has only low frequency components, so it will not significantly affect the high frequency accelerations of the handle.

By solving these two equations together, we can obtain the important transfer function from actuator force to handle acceleration, as follows:

$$H(s) = \frac{A_h(s)}{F_a(s)} = \frac{m_a s^4}{(m_a s^2 + b_s s + k_s)(m_h s^2 + b_{su} s + k_{su}) - (b_s s + k_s)^2} \quad (3)$$

Here, $b_{su} = b_s + b_u$ and $k_{su} = k_s + k_u$ for compactness. For typical parameter values, this fourth-order transfer function has four poles in the left half-plane and four zeros at the origin, giving a relative degree of zero. Different choices of the device parameters, such as k_s and m_h, will yield different pole locations, as will changes in the way the user is holding the handle, via k_u and b_u. However the zeros will always be at the origin, representing the fact that constant actuator forces are never observable from the handle acceleration sensor. The high frequency asymptote is a constant gain of $1/m_h$ with no phase lag, as the mass of the handle dominates at these frequencies. Having a model for these underlying dynamics helps one select system components for desirable performance. Once a system is constructed, standard system identification techniques can be used to verify the model's structure and find suitable values for its parameters.

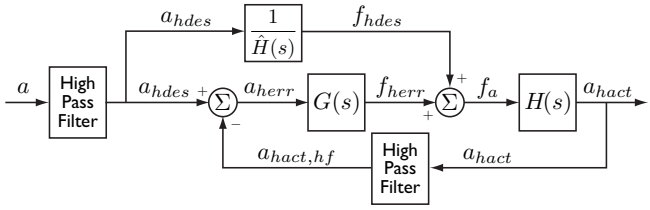

Fig. 2. Controller for matching the actual handle acceleration, a_{hact}, to a desired acceleration signal, a_{hdes}. The actuator force, f_a, includes a feedforward term, which seeks to invert the system's dynamics, and a feedback term, which aims to compensate for system variations and modeling inaccuracies.

B. Dynamic Compensation

The envisioned approach to providing realistic haptic feedback attaches a high-bandwidth linear actuator to the handle of a typical haptic interface. We want to use this actuator to make the handle accelerate in a specified way. Fig. 2 diagrams the proposed control architecture. Since an ungrounded force actuator cannot generate low frequency accelerations, we high-pass filter any acceleration command, a, passed to the system from a virtual or remote environment. The resulting desired handle acceleration, a_{hdes}, is then used to compute the actuator force, f_a, through a combination of feedforward and feedback. The feedforward term seeks to invert the system's dynamics, using the model $\hat{H}(s)$ to estimate the transfer function $H(s)$ discussed above. This open-loop feedforward term, f_{hdes}, is summed with a feedback term, f_{herr}, to yield the total force to be applied by the dedicated actuator. The feedback term is computed from the difference between the desired high frequency acceleration and a high-pass filtered version of the actual acceleration, which is measured by a sensor. In principle, this arrangement should enable the system to robustly output handle accelerations that closely track the command. The work described in this paper focuses on the influence of the dynamically compensated feedforward control term, and the use of feedback is left for future work.

Upon reexamination of $H(s)$ in (3), one notices that inversion will cause the four zeros at the origin to become four poles at the origin, which is a quadruple integrator. In other words, a naively inverted model will have infinite gain at steady-state and very high gain at low frequency, which will quickly saturate the actuator and prevent the system from functioning as intended. Thus, we need to be more careful in how we pick $\hat{H}(s)$. We seek to develop

Fig. 3. The haptic interface we developed to test the efficacy of the proposed approach. The standard stylus of a SensAble Phantom Omni was replaced with a custom handle for attachment of a dedicated vibration actuator and an accelerometer.

a model that captures the dynamics of our system in the frequency range of interest (20 Hz to 1000 Hz), but it needs to have finite (preferably large) gain at low frequency, so that its inverse will have finite (preferably small) gain at low frequency. The simplest dynamic model one could pick to satisfy these requirements is the mass m_h, which governs the system's high frequency asymptote. Dynamically compensated feedforward would consist of multiplying the desired acceleration by a constant gain, which is exactly what was done by Kontarinis and Howe [12]. However, this model is not expressive enough to capture the amplitude and phase changes that occur near resonance, leading us to pursue other techniques. As discussed for our specific system below, one can design a fourth-order dynamic model that has four low frequency zeros away from the origin, along with four carefully chosen poles, to yield a dynamic model that approximates our real system's behavior for the specified range of frequencies.

IV. IMPLEMENTATION

As an initial test for the approach described above, we created an *active handle for haptic display of realistic tool-mediated contact accelerations*. For this initial prototype, we focused on recreating the contact accelerations that are aligned with the main axis of the handle. When a real tool tip is dragged across a textured surface, it experiences significant accelerations in this direction.

A. Haptic Interface

As shown in Fig. 3, the prototyped device uses the NCM02-05-005-4JB linear voice coil actuator from H2W Technologies, Inc. This bidirectional actuator has the rated strength (2.2 N continuous and 6.6 N peak) and electrical bandwidth (3 kHz) to reproduce the texture accelerations present in tool-mediated exploration of surfaces. It also has a weight (30.2 g total mass) and form factor (13.2 mm diameter) suitable for mounting in a small handle. As with other voice coil actuators, the linear mapping from current to force (2.4 N/A) facilitates real-time use in a haptic interface.

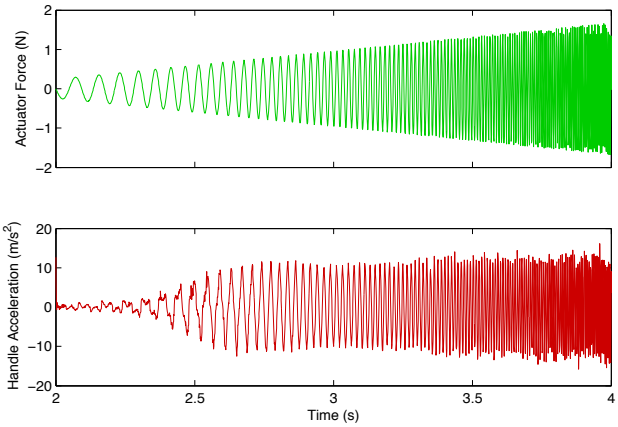

Fig. 4. Sample time-domain data from identification of the system shown in Fig. 3. The input is a linearly growing swept sinusoid for actuator force, f_a, and the measured output is the handle acceleration, a_h.

This actuator consists of an electromagnetic coil positioned around a permanent magnet core; these components are free to slide relative to each other along a low-friction jeweled sapphire linear bearing. For our device, we rigidly connected the magnet to the handle and used a pair of compression springs to center the movable coil in the actuator's workspace. This design allows easy modification of the spring constant, k_s, by replacement of the springs. The vibration actuator is driven by a high-bandwidth linear current amplifier.

Acceleration of the handle is measured by an Analog Devices ADXL320J accelerometer on a custom printed circuit board that is rigidly mounted to the handle. This accelerometer has a range of ± 5 g (± 49 m/s^2) and has been augmented with an on-board analog first-order low-pass filter with a cutoff frequency of 500 Hz, which prevents signal aliasing during analog-to-digital measurements. In order to measure position and velocity of the device as well as to enable the application of low frequency forces, we mounted the active handle to the Phantom Omni, a haptic interface commercially available from SensAble Technologies, Inc. This combination creates a haptic device that can display both high frequency contact accelerations, through our handle's dedicated vibration actuator, and low frequency force feedback, through the Omni's motors. This haptic interface is controlled via a Windows PC running a servo loop at 1 kHz. We use a Sensoray 626 card to both sample the accelerometer via a 16-bit ADC input and drive the actuator via a 14-bit DAC output.

B. System Identification

With the active handle system designed and assembled, we need to test the fourth-order model developed above for validity and fit its parameters to this specific hardware. The system was identified using frequency-domain techniques. While a user was holding the device's handle, the voice coil actuator repeatedly output a swept sinusoid in force. As shown in Fig. 4, this sinusoid was programmed to logarithmically sweep from 10 Hz to 200 Hz over the course of 2 s, starting at an amplitude of ± 0.24 N and linearly increasing to an amplitude of ± 1.68 N. This coupling of

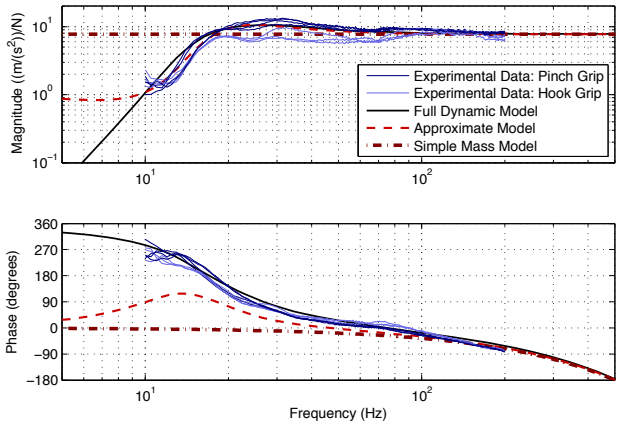

Fig. 5. Frequency-domain identification of the transfer function from actuator force to handle acceleration, $H(s) = A_h(s)/F_a(s)$. The three dynamic models were fit to the experimental data from the pinch grip tests.

TABLE I

PARAMETERS OF THE DYNAMIC MODEL SHOWN IN FIG. 1, AS IDENTIFIED FOR THE HARDWARE SYSTEM SHOWN IN FIG. 3.

Parameter	Value	Parameter	Value
m_a	0.018 kg	m_h	0.128 kg
k_s	266 N/m	k_u	1500 N/m
b_s	2 N/(m/s)	b_u	11 N/(m/s)
τ_d	0.001 s		

amplitude and frequency was used to prevent the actuator from hitting the limits of its travel ($\pm$3.8 mm), as spring deflections are large for low frequency force inputs.

Two users each performed four data collection trials for the system identification process. For two of these trials, the user pinched the wooden part of the device's handle with his or her index finger, middle finger and thumb. For the other two, the user hooked his or her fingers around the bottom of the stylus and held the immobilized gimbal joints. The swept sinusoid was repeated three times during each trial, and the vertical handle acceleration was recorded. For all trials, the user attempted to maintain a moderate grip force and did not make any purposive motions. The second and third sinusoid were segmented out of each trial, and the collected data were analyzed in the frequency domain, as done in [15], [13]. The discrete Fourier transform (DFT) of the output (a_h) was divided by the DFT of the input (f_a) to yield the experimental transfer function estimates shown in Fig. 5. The system's behavior was quite consistent across users and trials. However, the four tests done with the pinch grip are more similar to one another than they are to the test performed with the hook grip. This observation suggests that grip configuration has a deterministic effect on the behavior of the system across users.

The pinch grip experimental transfer function estimates shown in Fig. 5 were used to guide the selection of parameters for the parametric dynamic model given by (3). The mass of the moving part of the actuator, m_a, and the stiffness of the springs, k_s, were known from manufacturer specifications. The mass of the handle, m_h, represents the remainder of the actuator's mass, the effective endpoint mass of the Omni, and the additional mass coupled in by the user's hand. This parameter was empirically tuned, along with the other remaining parameters, to reach the values shown in Table I. The parameter τ_d is the constant time delay associated with $H(s)$, the transfer function from f_a to a_h; this one millisecond time delay is primarily due to the 1000 Hz discrete-time implementation of our servo loop. The model's response with this set of parameters is illustrated with the full dynamic model trace in Fig. 5; the good match verifies the structure of the model. A simple mass model and an approximate dynamic model were designed for use in the controller in order to try to capture the behavior of the system above 20 Hz. The mass of the simple model is 0.128 kg, matched to m_h in the full model. The approximate model has pairs of complex zeros at 9 Hz and 12 Hz with $\zeta = 0.5$ and 0.3 respectively; pairs of complex poles at 15 Hz and 20 Hz with $\zeta = 0.35$ and 0.4 respectively; and a DC gain of 1.0. While neither of these models captures the full behavior observed in the experimental data, both have the correct high frequency magnitude asymptote, and their performance will be compared quantitatively in the following section.

V. TELEOPERATION EXPERIMENT

In order to test how capable our prototype is at displaying realistic contact accelerations, we developed a master-slave teleoperation experiment that allows us to derive in real-time a desired acceleration signal for the master handle from *real* tool accelerations measured from a slave end-effector. This experiment also gives us an opportunity to demonstrate an application for our approach, *high frequency acceleration matching of teleoperated tools*.

A. Setup

The teleoperation experiment utilizes a second Omni to act as the slave robot. As shown in Fig. 6, the stylus of the slave Omni is instrumented with an ADXL320J accelerometer that has an on-board analog low-pass filter at 500 Hz. We use a Windows PC and a Sensoray 626 card to implement a 1 kHz servo loop that both controls the actuator on the master handle and provides position-position control of the two Omnis (k_m = k_{sl} = 0.25 N/mm), as diagrammed in Fig. 7. The non-actuated joints (gimbals) of both Omnis are immobilized so that there is a one-to-one mapping between the position of the active handle of the master and the tip of the stylus of the slave. In our experiments, a user holding the master Omni's handle uses the slave Omni's tool tip to perform exploratory dragging motions across a sample surface. We tested the three sample surfaces shown in Fig. 8: unfinished plywood, black plastic embossed text, and gray textured vinyl.

For the task of acceleration matching, we tested the performance of three different controllers: *None*, *constant gain*, and *dynamically compensated*. *None* provides a baseline measurement of the performance of the position-position controller without use of the dedicated actuator; it represents the traditional approach to haptic feedback, where position commands and virtual springs are tasked with conveying the feel of the virtual or remote object being touched. The other two controllers use the actuator to attempt to make

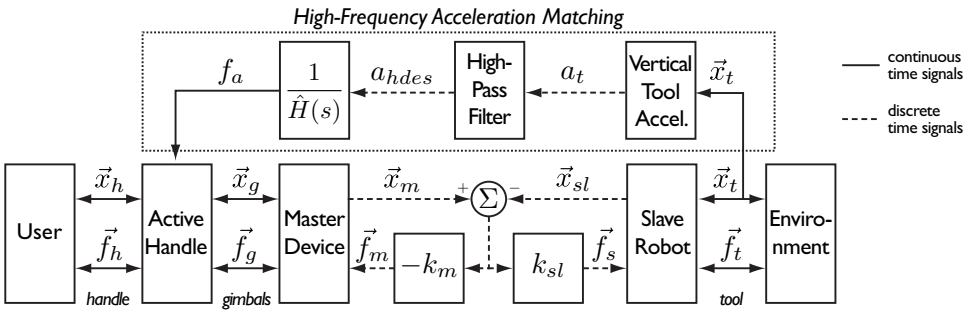

Fig. 7. Block diagram for position-position teleoperation with an auxiliary channel for recreating the slave tool accelerations with a dedicated handle actuator. This implementation uses only an open-loop feedforward inversion of the system's identified dynamics, without closed-loop feedback on the actual handle acceleration. Choosing different forms for the model $\hat{H}(s)$ results in a variety of controllers that can be compared.

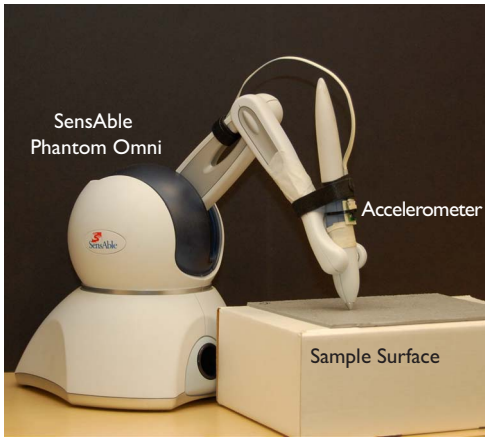

Fig. 6. The slave robot used in the teleoperation experiment.

Fig. 8. The three surfaces that were tested with the teleoperation system: unfinished plywood, hard plastic embossed with text, and textured vinyl.

the high frequency accelerations of the master handle match those of the slave tip. For each of these, the desired handle acceleration, a_{hdes}, is computed by sending the measured slave tool acceleration, a_t, through a fourth-order Butterworth high-pass filter with a cutoff frequency of 15 Hz. This filter prevents the system from attempting to recreate the low frequency accelerations that stem from the user's own vertical hand motions, and it attenuates the gain of the inverse models at low frequency to prevent the actuator from reaching its limits.

For *constant gain* control, the desired acceleration signal, a_{hdes}, is multiplied by a scalar gain (0.128 N/(m/s^2) = 0.128 kg) to calculate f_a, the acceleration command signal that drives the linear actuator. This control mode corresponds with the simple mass model described in Section IV-B and is similar to the approach taken by Kontarinis and Howe [12]. With our dynamically compensated control, the desired acceleration a_{hdes} is passed through the inverse of the approximate dynamic model (described in Section IV-B) to determine the appropriate actuator command.

B. Results and Discussion

The time domain acceleration data for the experiments are shown in Fig. 9. These results show both the accelerations that were sensed at the slave tool and the accelerations that were felt by the user through the handle of the haptic interface. Note that the signals in these plots and in the analyses below have been shifted to eliminate the 0.001 s time delay (τ_d) that exists between the slave and the master. Visually we see that both the *constant gain* and *dynamic compensation* controllers are much more capable of providing high frequency feedback than the *none* controller (naive position control).

To quantify this improvement, we calculated the root mean square error between the time-shifted master handle acceleration, a_{hact}, and the desired handle acceleration, a_{hdes}, for each test. As shown in Table II, we normalize these RMS error values by the RMS of the command signal to control for trial-to-trial variations due the human operator. Without use of the dedicated actuator, the acceleration felt by the user has an average normalized RMS error of 99.5%, i.e., the user cannot feel the high frequency accelerations that the slave tool is experiencing. Constant gain acceleration feedback reduces this value to 79.1% error, and the dynamically compensated controller brings it down to 72.0% error. Note that RMS error is a stringent metric that penalizes both magnitude and phase differences; the level to which RMS error must be reduced to make two acceleration signals feel identical has yet to be determined. Thus, we also explored other performance metrics.

Fig. 10 shows linear regression analyses between the time-shifted master handle acceleration and the desired handle acceleration for all nine tests, where each point represents a single time sample. Each plot is annotated with the least squares fit line, its equation, the R^2 value, and a reference line showing perfect acceleration matching. Not surprisingly, the controller without acceleration feedback shows no correlation. Both the constant gain and the dynamically compensated acceleration controllers show a strong positive correlation. The average slope of the constant gain fits is 0.60 with an average R^2 value of 0.65, and the average slope of

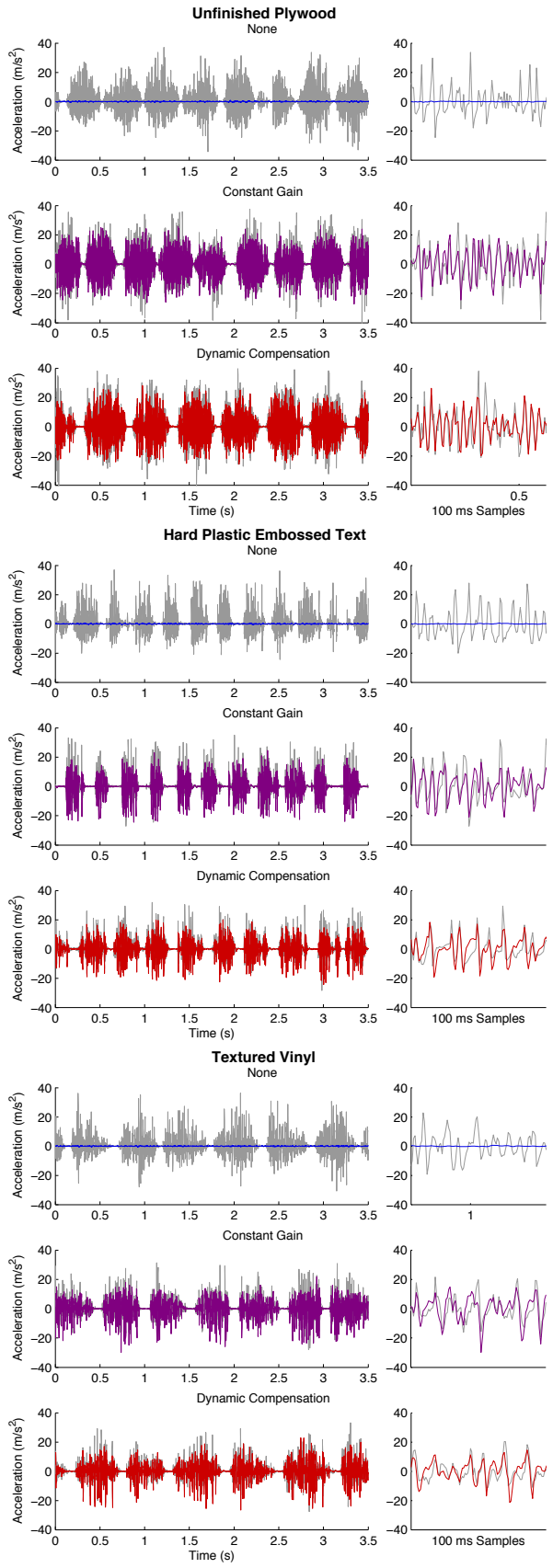

Fig. 9. Desired and actual acceleration for the teleoperation experiments with the three tested controllers. Desired accelerations are shown in gray.

the dynamically compensated fits is 0.64 with an average R^2 value of 0.71. Having slopes less than unity indicates that these controllers are generally under-actuating the handle.

Lastly, Fig. 11 shows an analysis of the frequency spectra of the high-pass filtered master and slave accelerations. The handle experiences minimal high frequency accelerations without use of the dedicated actuator. Both active handle controllers exhibit similarly shaped spectra up to approximately 300 Hz for all three surface samples. This result indicates that both of these controllers are capable of producing accelerations that have approximately the same frequency content as their command signals.

Overall, the constant gain and dynamic compensation controllers behave similarly, with dynamic compensation slightly outperforming constant gain on each of the quantitative metrics that we tested. However this difference has not yet been tested for statistical or perceptual significance.

VI. CONCLUSIONS

Experiments with an initial prototype have provided encouraging results for our approach with regard to both the qualitative feel of the haptic interaction and the quantitative performance of matching realistic contact accelerations from a slave robot. This paper focused exclusively on the influence of dynamic compensation in the acceleration output controller; future work will augment this feedforward approach by closing the loop on acceleration output. We also believe that increasing the speed of the servo loop will allow us to produce high frequency accelerations with greater fidelity. Finally, we would like to do human subject experiments to study the perceptual requirements for discrimination of realistic contact accelerations, as well as the potential benefits this approach may have on common applications for haptic interfaces.

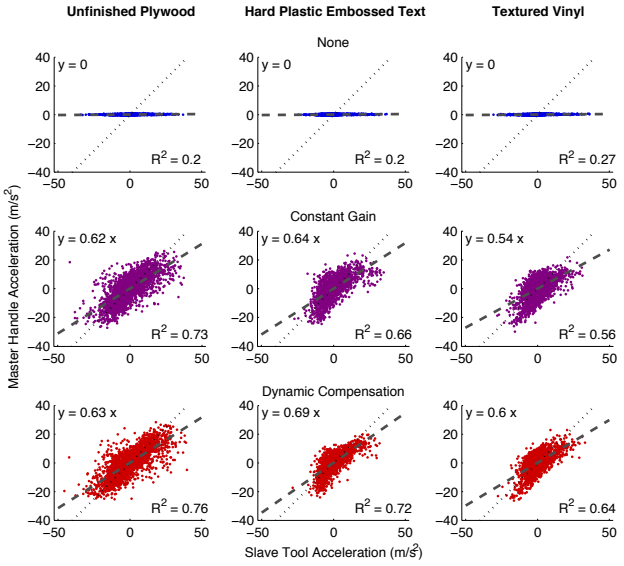

Fig. 10. Linear regressions between slave and master acceleration signals.

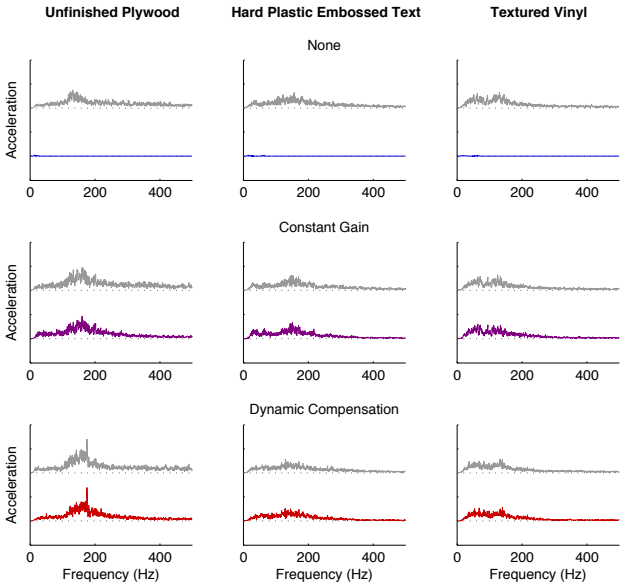

Fig. 11. Discrete Fourier transforms of slave and master accelerations; slave accelerations are shown in gray.

TABLE II

ROOT MEAN SQUARE ERROR IN HANDLE ACCELERATION, NORMALIZED BY THE ROOT MEAN SQUARE OF THE DESIRED ACCELERATION SIGNAL.

	Plywood	Text	Vinyl	Average
None	99.6	99.5	99.3	99.5
Constant Gain	69.8	80.6	92.3	79.1
Dynamically Compensated	65.1	73.2	82.8	72.0

VII. ACKNOWLEDGMENTS

The authors thank the other members of the Penn Haptics Lab for sharing their thoughts and insights on this work.

REFERENCES

[1] J. Bell, S. Bolanowski, and M. H. Holmes. The structure and function of Pacinian corpuscles: A review. *Progress in Neurobiology*, 42(1):79–128, Jan. 1994.

[2] J. E. Colgate, M. C. Stanley, and G. Schenkel. Dynamic range of achievable impedances in force reflecting interfaces. In *Proc. SPIE Telemanipulator Technology and Space Telerobotics Conference*, volume 2057, pages 199–210, Boston, Massachusetts, September 1993.

[3] D. Constantinescu, S. E. Salcudean, and E. A. Croft. Haptic rendering of rigid body contacts using impulsive and penalty forces. *IEEE Transactions on Robotics*, pages 309–323, June 2005.

[4] R. Daniel and P. McAree. Fundamental limits of performance for force reflecting teleoperation. *Int. Journal of Robotics Research*, 17(8):811–830, Aug. 1998.

[5] J. T. Dennerlein, P. A. Millman, and R. D. Howe. Vibrotactile feedback for industrial telemanipulators. In *Sixth Annual Symposium on Haptic Interfaces for Virtual Environments and Teleoperator Systems*, Nov. 1997.

[6] N. Diolaiti, G. Niemeyer, F. Barbagli, and J. K. Salisbury. Stability of haptic rendering: Discretization, quantization, time delay, and Coulomb effects. *IEEE Transactions on Robotics*, 22(2):256–268, Apr. 2006.

[7] J. P. Fiene and K. J. Kuchenbecker. Shaping event-based haptic transients via an improved understanding of real contact dynamics. In *Proc. IEEE World Haptics Conference*, pages 170–175, March 2007.

[8] S. Greenish, V. Hayward, V. Chial, A. M. Okamura, , and T. Steffen. Measurement, analysis and display of haptic signals during surgical cutting. *Presence*, 11(6):626–651, 2002.

[9] M. Hollins and S. R. Risner. Evidence for the duplex theory of tactile texture perception. *Perception and Psychophysics*, 62(4):695–705, May 2000.

[10] R. L. Klatzky and S. J. Lederman. *Haptic Rendering: Algorithms and Applications*, chapter 1: Perceiving Object Properties Through A Rigid Link. A. K. Peters, 2008.

[11] D. Kontarinis, J. Son, W. Peine, and R. Howe. A tactile shape sensing and display system for teleoperated manipulation. In *Proc. IEEE International Conference on Robotics and Automation*, pages 641–646, May 1995.

[12] D. A. Kontarinis and R. D. Howe. Tactile display of vibratory information in teleoperation and virtual environments. *Presence: Teleoperators and Virtual Environments*, 4(4):387–402, Aug. 1995.

[13] K. J. Kuchenbecker, J. P. Fiene, and G. Niemeyer. Improving contact realism through event-based haptic feedback. *IEEE Transactions on Visualization and Computer Graphics*, 12(2):219–230, March/April 2006.

[14] K. J. Kuchenbecker and G. Niemeyer. Improving telerobotic touch via high-frequency acceleration matching. In *Proc. IEEE International Conference on Robotics and Automation*, pages 3893–3898, May 2006.

[15] K. J. Kuchenbecker, J. G. Park, and G. Niemeyer. Characterizing the human wrist for improved haptic interaction. In *Proc. ASME International Mechanical Engineering Congress and Exposition, Symposium on Advances in Robot Dynamics and Control*, volume 2, paper number 42017, Nov. 2003.

[16] R. H. LaMotte. Softness discrimination with a tool. *Journal of Neurophysiology*, 83:1777–1786, 2000.

[17] J. C. Lee, P. H. Dietz, D. Leigh, W. S. Yerazunis, and S. E. Hudson. Haptic pen: A tactile feedback stylus for touch screens. In *Proc. ACM Symposium on User Interface Software and Technology*, volume 6, pages 291–294, October 2004.

[18] C. Liao, F. Guimbretiere, and C. E. Loeckenhoff. Pen-top feedback for paper-based interfaces. In *Proc. ACM Symposium on User Interface Software and Technology*, pages 201–210, 2006.

[19] J. M. Loomis. Distal attribution and presence. *Presence: Teleoperators and Virtual Environments*, 1(1):113–119, 1992.

[20] J. M. Loomis and S. J. Lederman. Tactual perception. In K. R. Boff, L. Kaufman, and J. P. Thomas, editors, *Handbook of Perception and Human Performance*, volume II: Cognitive Processes and Performance, chapter 31. John Wiley and Sons, 1986.

[21] A. M. Okamura, M. R. Cutkosky, and J. T. Dennerlein. Reality-based models for vibration feedback in virtual environments. *IEEE/ASME Transactions on Mechatronics*, 6(3):245–252, Sept. 2001.

[22] A. M. Okamura, J. T. Dennerlein, and R. D. Howe. Vibration feedback models for virtual environments. In *Proc. IEEE International Conference on Robotics and Automation*, volume 3, pages 674–679, May 1998.

[23] K. Salisbury, D. Brock, T. Massie, N. Swarup, and C. Zilles. Haptic rendering: Programming touch interaction with virtual objects. In *Proceedings of the Symposium on Interactive 3D Graphics*, pages 123–130. ACM, 1995.

[24] S. A. Wall and W. Harwin. A high bandwidth interface for haptic human computer interaction. *Mechatronics*, 11(4):371–387, June 2001.

[25] S. A. Wall and W. S. Harwin. Effects of physical bandwidth on perception of virtual gratings. In *Proc. ASME Int. Mechanical Engineering Congress and Exposition*, pages 1033—1047, 2000.

[26] P. Wellman and R. D. Howe. Towards realistic vibrotactile display in virtual environments. In *Proc. ASME Dynamic Systems and Control Division*, volume 57, pages 713–718, 1995.

[27] H.-Y. Yao, V. Hayward, and R. E. Ellis. A tactile enhancement instrument for minimally invasive surgery. *Computer-Aided Surgery*, 10(4):233–239, 2005.